

# Simulation of electrostatically driven jets from non-viscous drops using Level Sets

Maria Garzón, Len Gray and James Sethian

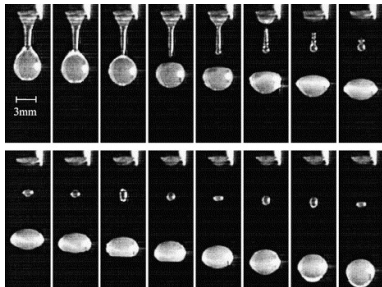
July 4, 2012 FBP 2012 Germany

# Plan

1. Motivation examples
2. The mathematical model.
3. The Level Set formulation.
4. The numerical approximation.
5. Numerical results
  - ▶ Oscillation sphere,  $E_\infty = 0$ .
  - ▶ Drop distortion,  $E_\infty \neq 0$
  - ▶ Jetting details.

# Motivation examples

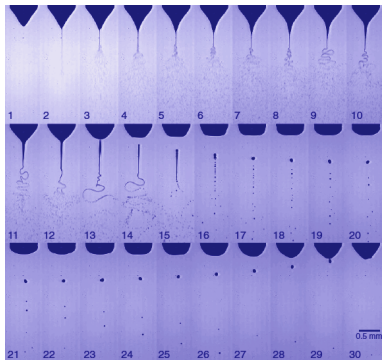
## Dripping faucet



T=23.5°C  
p=50.8 bar

liquid: ethanol  
gas: nitrogen  
frequency: 562½ Hz

## Electrospraying



Inviscid, incompressible fluid  $\Rightarrow$  Potential flow.

Uniform electric field  $\Rightarrow$  Electrostatic field.

Moving boundaries:

1. The free boundary can change topology  $\rightarrow$  Level Set Method
2. The BC on the free boundary is a PDE  $\rightarrow$  Level Set Method

# Motivation examples



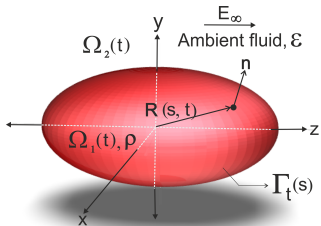
Spraying regimes:

- Spindle mode
- Pulsating Taylor cone mode
- Cone-jet mode
- Multijet emission mode

Previous relevant works:

- ▶ Basaran et all, 1995
- ▶ Lopez-Herrera et all, 2004
- ▶ Fontelos et all, 2008
- ▶ Grimm and Beauchamp, 2005
- ▶ Marginean et all, 2006

# The model assumptions



$u(x, y, z, t)$ , Fluid velocity field  
 $\phi(x, y, z, t)$ , Velocity potential  
 $p(x, y, z, t)$ , Pressure field  
 $U(x, y, z, t)$ , Electric potential  
 $\rho, \gamma, \epsilon$ , Fluid density, surface tension coefficient, permittivity  
 $\kappa = \frac{1}{R_1} + \frac{1}{R_2}$ , Twice mean curvature

- ▶ A perfectly conducting liquid droplet, initially of spherical shape, immersed in an unlimited gaseous dielectric (permittivity  $\epsilon$ ), exposed to an external uniform electric field  $\mathbf{E}_\infty$
- ▶ The ambient medium is uniform and uncharged, the electric potential  $U$  is governed by the Laplace equation.
- ▶ Inviscid fluid droplet of density  $\rho$ . Potential flow for the interior fluid dynamics, the exterior fluid is dynamically at rest.

# The model equations

$$\begin{aligned}\mathbf{u} &= \nabla\phi && \text{in } \Omega_1(t) \\ \Delta\phi &= 0 && \text{in } \Omega_1(t) \\ \rho\frac{\partial\phi}{\partial t} + \frac{1}{2}|\nabla\phi|^2 + \frac{p}{\rho} &= 0 && \text{in } \Omega_1(t) \\ \Delta U &= 0 && \text{in } \Omega_2(t)\end{aligned}$$

The pressure jump across  $\Gamma_t(\mathbf{s})$ :  $p = p_a + \gamma\kappa - \frac{\epsilon}{2}|\nabla U \cdot \mathbf{n}|^2$

- ▶ Boundary conditions for the fluid problem:

$$\begin{aligned}D_t\mathbf{R} &= \mathbf{u} \quad \text{on } \Gamma_t(\mathbf{s}) \\ \rho\left(\frac{\partial\phi}{\partial t} + \frac{1}{2}|\nabla\phi|^2\right) + \gamma\kappa - \frac{\epsilon}{2}|\nabla U \cdot \mathbf{n}|^2 &= 0 \quad \text{on } \Gamma_t(\mathbf{s})\end{aligned}$$

- ▶ Boundary conditions for electric field problem:

$$\begin{aligned}U &= U_0 \quad \text{on } \Gamma_t(\mathbf{s}) \\ U &= -E_\infty z \quad \text{at the far field.}\end{aligned}$$

Perfect conducting surface  $\Rightarrow U = U_0$  on  $\Gamma_t(\mathbf{s})$ .

The value of  $U_0$  at each time step is calculated imposing:

$$\begin{cases} \int_{\Gamma_t(\mathbf{s})} \frac{\partial U}{\partial n} d\Gamma = 0, & \text{for uncharged drops} \\ \int_{\Gamma_t(\mathbf{s})} \frac{\partial U}{\partial n} d\Gamma = q, & \text{for charged drops} \end{cases}$$

We make the **change of variable**:  $U = \tilde{U} + E_\infty z$ , and then  $\tilde{U} = 0$  at infinity and  $\tilde{U}|_{\Gamma_t(\mathbf{s})} = -E_\infty z + U_0$ .

For a single drop:

$$\text{Let be } \begin{cases} \tilde{U}_n^z & \text{the flux from bound. cond. } \tilde{U} = -E_\infty z \\ \tilde{U}_n^1 & \text{the flux from bound. cond. } \tilde{U} = 1 \end{cases}$$

$$\int_{\Gamma_t(\mathbf{s})} \tilde{U}_n^z d\Gamma + U_0 \int_{\Gamma_t(\mathbf{s})} \tilde{U}_n^1 d\Gamma = -E_\infty \int_{\Gamma_t(\mathbf{s})} n_z d\Gamma \Rightarrow U_0 \text{ (uncharged)}$$

$$\int_{\Gamma_t(\mathbf{s})} \tilde{U}_n^z d\Gamma + U_0 \int_{\Gamma_t(\mathbf{s})} \tilde{U}_n^1 d\Gamma = q - E_\infty \int_{\Gamma_t(\mathbf{s})} n_z d\Gamma \Rightarrow U_0 \text{ (charged)}$$

## Characteristic scales :

$$\begin{cases} r_0 & \text{Initial droplet radius} \\ \sqrt{\frac{\rho r_0^3}{\gamma}} & \text{Capillary time} \\ \sqrt{\frac{2\gamma}{\epsilon r_0}} & \text{Electrical field} \end{cases}$$

All the equations in dimensionless form remains the same, except:

$$\frac{\partial \phi}{\partial t} + \frac{1}{2} |\nabla \phi|^2 + \kappa - |\nabla U \cdot \mathbf{n}|^2 = 0 \quad \text{on } \Gamma_t(\mathbf{s})$$

which can be rearranged

$$\frac{\partial \phi}{\partial t} + \mathbf{u} \cdot \nabla \phi = f$$

$$f = \frac{1}{2} (\mathbf{u} \cdot \mathbf{u}) - \kappa + |\nabla U \cdot \mathbf{n}|^2$$

And the only parameter left in the model is the non dimensional electric field strength at the far field:

$$E_\infty$$



Therefore, the model equations in 3D are:

$$\mathbf{u} = \nabla\phi \text{ in } \Omega_1(t)$$

$$\Delta\phi = 0 \text{ in } \Omega_1(t)$$

$$D_t\mathbf{R} = \mathbf{u} \text{ on } \Gamma_t(\mathbf{s})$$

$$D_t\phi = f \text{ on } \Gamma_t(\mathbf{s})$$

$$\Delta U = 0 \text{ in } \Omega_2(t)$$

$$U = U_0 \text{ on } \Gamma_t(\mathbf{s})$$

$$U = -E_\infty z \text{ at the far field}$$



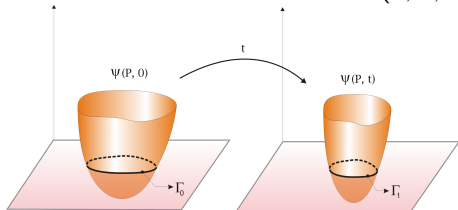
### Eulerian-Lagrangian formulation

Classical methods: **Front tracking methods** suffers difficulties when the free boundary changes topology.



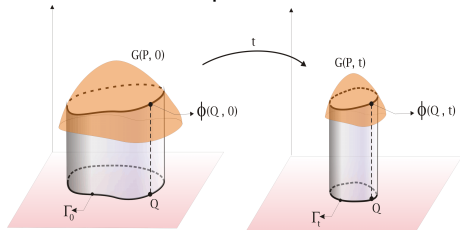
# The Level Set formulation in 2D

- ▶ The levelset function  $\Psi(r, z, t)$  on a fixed domain  $\Omega_D$



$$\Psi(\mathbf{R}(s, t), t) = 0, \quad \forall t$$

- ▶ The fictitious potential function  $G(r, z, t)$  on  $\Omega_D$



$$G(\mathbf{R}(s, t), t) = \phi(r, z, t) |_{\Gamma_t(s)} = \Phi(s, t), \quad \forall t$$

► Differentiating both equations with respect to  $t$

$$\begin{aligned}\Psi_t + \mathbf{u} \cdot \nabla \Psi &= 0 \text{ on } \Gamma_t(s). \\ D_t \Phi = G_t + \mathbf{u} \cdot \nabla G &= f \text{ on } \Gamma_t(s).\end{aligned}$$

being

$$f = \frac{1}{2}(\mathbf{u} \cdot \mathbf{u}) - \kappa + |\nabla U \cdot \mathbf{n}|^2$$

Define  $\mathbf{u}_{\text{ext}}, f_{\text{ext}}$  on  $\Omega_D$  such that 
$$\begin{cases} \mathbf{u}_{\text{ext}}|_{\Gamma_t(s)} = \mathbf{u}(\mathbf{R}(s, t), t) \\ f_{\text{ext}}|_{\Gamma_t(s)} = f(\mathbf{R}(s, t), t) \end{cases}$$

$$\begin{array}{l} \boxed{D_t \mathbf{R} = \mathbf{u} \text{ on } \Gamma_t(s)} \rightarrow \boxed{\Psi_t + \mathbf{u}_{\text{ext}} \cdot \nabla \Psi = 0 \text{ in } \Omega_D} \\ \boxed{D_t \phi = f \text{ on } \Gamma_t(s)} \rightarrow \boxed{G_t + \mathbf{u}_{\text{ext}} \cdot \nabla G = f_{\text{ext}} \text{ in } \Omega_D} \end{array}$$

**Remark:**  $\mathbf{u}_{\text{ext}}$ , and  $f_{\text{ext}}$  are obtained as in (Adals., Sethian, 1999)

The model equations in **Eulerian formulation** are:

$$\mathbf{u} = \nabla\phi \text{ in } \Omega_1(t) \quad (8)$$

$$\Delta\phi = 0 \text{ in } \Omega_1(t) \quad (9)$$

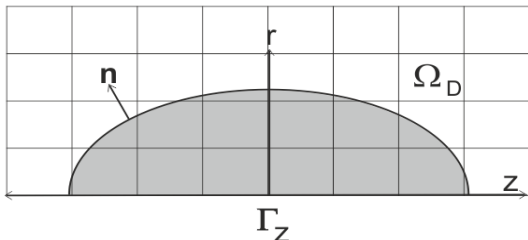
$$\Psi_t + \mathbf{u}_{\text{ext}} \cdot \nabla\Psi = 0 \text{ in } \Omega_D \quad (10)$$

$$G_t + \mathbf{u}_{\text{ext}} \cdot \nabla G = f_{\text{ext}} \text{ in } \Omega_D \quad (11)$$

$$\Delta U = 0 \text{ in } \Omega_2(t) \quad (12)$$

$$U = U_0 \text{ on } \Gamma_t(s) \quad (13)$$

$$U = -E_\infty z \text{ at the far field} \quad (14)$$



$$\text{On } \Gamma_z : u = 0; \quad \frac{\partial\phi}{\partial n} = 0; \quad \frac{\partial\Psi}{\partial n} = 0; \quad \frac{\partial G}{\partial n} = 0; \quad \frac{\partial U}{\partial n} = 0.$$

**Remark:** System (8-14) is equivalent to (1-7) (proof in M.G. et al, 2009)

# The numerical approximation

► Time Discretization:

$$\mathbf{u}^n = \nabla \phi^n \text{ in } \Omega_1(t_n) \quad (15)$$

$$\Delta \phi^n(r, z) = 0 \text{ in } \Omega_1(t_n) \quad (16)$$

$$\frac{\Psi^{n+1} - \Psi^n}{\Delta t} = -\mathbf{u}_{\text{ext}}^n \cdot \nabla \Psi^n \text{ in } \Omega_D \quad (17)$$

$$\frac{G^{n+1} - G^n}{\Delta t} = -\mathbf{u}_{\text{ext}}^n \cdot \nabla G^n + f_{\text{ext}}^n \text{ in } \Omega_D, \quad (18)$$

$$\Delta U^n(r, z) = 0 \text{ in } \Omega_2(t_n) \quad (19)$$

► Space Discretization:  $G_{i,j}^n \approx G(r_i, z_j, t_n)$ ,  $\mathbf{u}_{\text{ext}}^n = (u^n, v^n)$ .

A **first order upwind** scheme for Eq. (18) is:

$$\begin{aligned} G_{i,j}^{n+1} &= G_{i,j}^n - \Delta t (\max(u_{i,j}^n, 0) D_{i,j}^{-r} + \min(u_{i,j}^n, 0) D_{i,j}^{+r} \\ &+ \max(v_{i,j}^n, 0) D_{i,j}^{-z} + \min(v_{i,j}^n, 0) D_{i,j}^{+z}) + \Delta t f_{i,j}^n, \end{aligned}$$

We have to add the discretize BC for each particular case.

- ▶ At each  $t_n$ , the two Laplace eqn.:

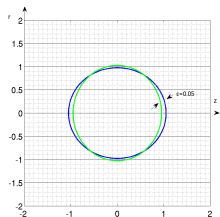
$$\begin{cases} \Delta\phi = 0 & \text{subject to } \phi = G^n & \text{on } \Gamma_t(s) \\ \Delta U = 0 & \text{subject to } U = U_0^n & \text{on } \Gamma_t(s) \end{cases}$$

have to be solved:

- ▶ We use a Boundary Integral formulation for both problems and the **linear BEM** approximation.
- ▶ For the electric potential problem the **BEM matrices** calculated to solve the fluid problem can be **reused**. The computational expense is very reasonable.

Details in Garzon et al, 2011.

# The oscillating sphere, $E_\infty = 0$



$$\phi(r, z, 0) = 0$$

$$z(s) = -\cos(s) (1 + \epsilon P_m(\cos(s)))$$

$$r(s) = \sin(s) (1 + \epsilon P_m(\cos(s)))$$

$$0 \leq s \leq \pi, \quad \epsilon \ll 1$$

$$\omega^2 = \frac{m(m-1)(m+2)}{m+1}$$

- $\epsilon = 0.05$ ,  $\Omega_D = [-2, 2] \times [-2, 2]$ ,  $m = 2$ .

Discretization parameters

$$\begin{cases} \Delta r = \Delta z & \text{for } \Omega_D \\ \Delta s = \frac{S}{N_p - 1} & \text{for } \Gamma_t(s) \\ \Delta t \leq \min\left(\frac{\Delta r}{|\mathbf{u}|_{\max}}, 0.2\Delta s^{3/2}\right) & \text{CFL, capillary wave scales} \end{cases}$$

- Several numerical tests to check convergence properties:

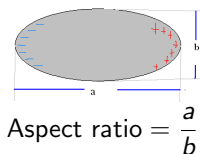
$$\begin{cases} e_T &= \left| \frac{T_c - T}{T} \right| \leq 1 \times 10^{-3} \\ e_V &= \left| \frac{V_f - V_0}{V_0} \right| \leq 1 \times 10^{-3} \\ e_\mathcal{E} &= \left| \frac{\mathcal{E}_f - \mathcal{E}_0}{\mathcal{E}_0} \right| \leq 7 \times 10^{-4} \end{cases}$$

First order convergence with respect to space (details in M.G. et al, 2011)



# Droplet distortions in electric fields, $E_\infty \neq 0$

- ▶ Neutral droplet,  $q = 0$



$$\tilde{E}_\infty^c = \frac{c}{\sqrt{8\pi}} \left( \frac{2\gamma}{\epsilon r} \right) \quad \text{Taylor limit}$$

$$E_\infty^c = 0.3241$$

Shapes became unstable.

Symmetrically elongated parallel to the electric field  $\Rightarrow$  **symmetric jet discharge**

- ▶ Charged droplet,  $q \neq 0$



$$E_\infty^c < \text{Taylor limit}$$

Shapes became unstable

Tear shaped drop  $\Rightarrow$  **Alternate jet discharge**

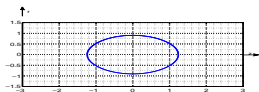
$$q > q_R$$

$$q_R = \frac{8\pi}{\gamma \epsilon r^3}$$

# Droplet distortion under electric field simulations

► Numerical tests for different  $E_\infty$  values:

- Sphere  $r = 1$ ,  $\phi(r, z, 0) = 0$ ,  $\Omega_D = [-3, 3] \times [-1.5, 1.5]$
- Discretization parameters:

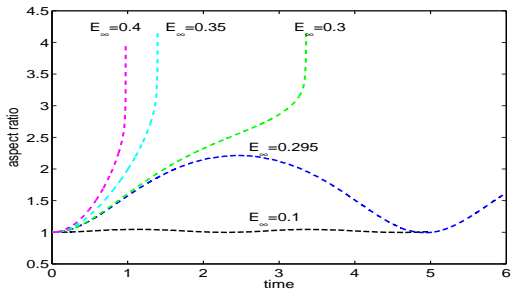
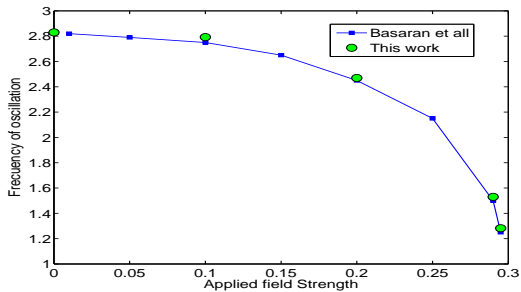


$$\begin{cases} \Delta r = \Delta z = 0.01 & \text{for } \Omega_D \\ \Delta s = 0.0157 - 0.03 & \text{for } \Gamma_t(s) \\ \Delta t = 0.001 - 2.5 \times 10^{-5} \end{cases}$$

$E_\infty$	$\omega$	Aspect ratio	$t_f$	$e_v$	$N_{\text{steps}}$
0.1	2.8176	1.046	5.0	$7.6111 \times 10^{-4}$	5000
0.2	2.4513	1.256	5.0	$9.4912 \times 10^{-4}$	5000
0.295	1.2823	2.255	5.0	$5.8061 \times 10^{-3}$	5000
0.3		3.227	3.3562	$4.2511 \times 10^{-3}$	3454
0.35		3.051	1.3946	$3.4452 \times 10^{-3}$	1550
0.4		2.608	0.9707	$2.6446 \times 10^{-3}$	995

Table: Frequency of oscillation, aspect ratio, final time, relative error in volume and number of time steps

$E_\infty = 0.3$  Critical value

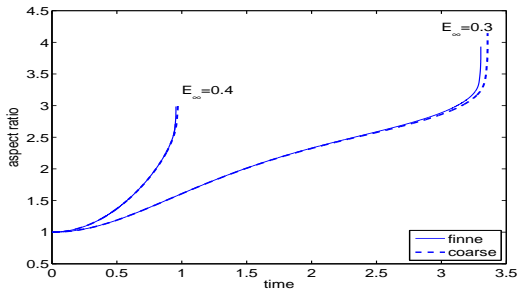


► Numerical tests to check **convergence** with respect discretization parameters :

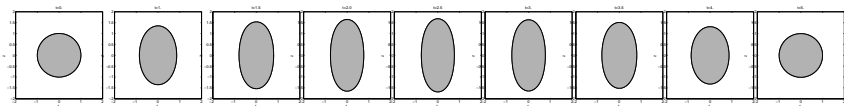
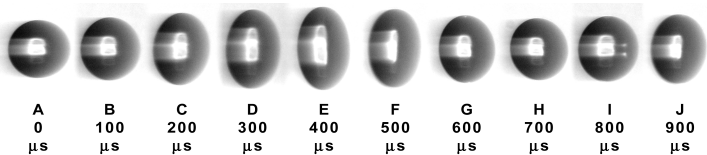
$$\left\{ \begin{array}{l} \Delta z = 0.010, N_p = 201, \Delta s \approx 0.033, \Delta t = 0.001 \text{ to } 0.0002 \rightarrow \textit{coarse grid} \\ \Delta z = 0.005, N_p = 301, \Delta s \approx 0.025, \Delta t = 0.0005 \text{ to } 0.0001 \rightarrow \textit{fine grid} \end{array} \right.$$

$E_\infty$	$t_f$ (coarse)	$t_f$ (fine)	$e_V$ (coarse)	$e_V$ (fine)
0.3	3.3562	3.3041	$4.2522 \times 10^{-3}$	$2.1381 \times 10^{-3}$
0.4	0.9707	0.9521	$2.6446 \times 10^{-3}$	$1.3195 \times 10^{-3}$

Table: Jetting time, relative error in volume and number of time steps

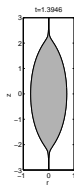
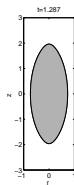
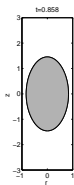
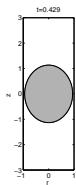


# Front profiles, $E_\infty = 0.295$

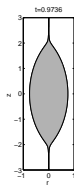
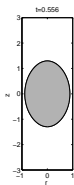
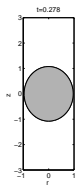


# Front profiles, $E_\infty = 0.35, 0.40$

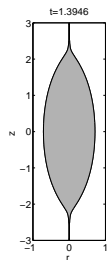
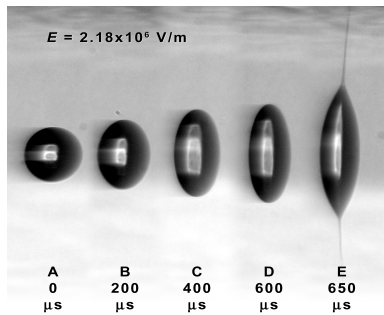
$E_\infty = 0.35$



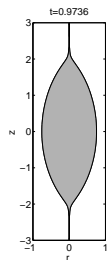
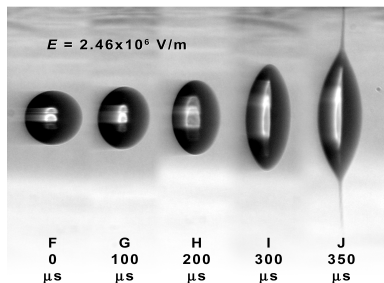
$E_\infty = 0.40$



# Front profiles and Lab Photos, $E_{\infty} = 0.35, 0.40$

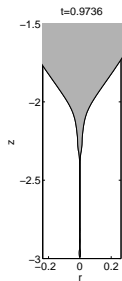
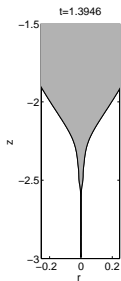


$$E_{\infty} = 0.35$$



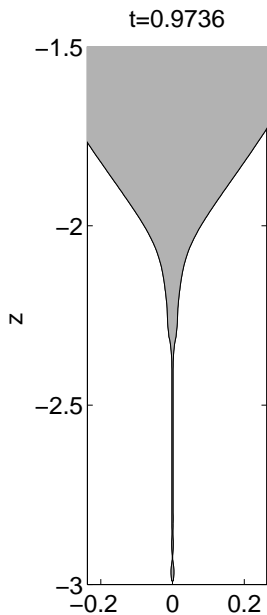
$$E_{\infty} = 0.40$$

Front profiles zoomed,  $E_\infty = 0.35, 0.40$

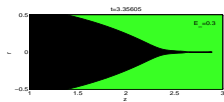
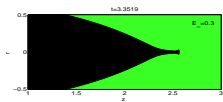
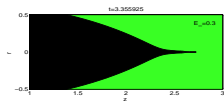
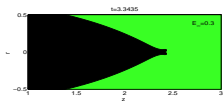
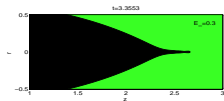
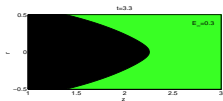
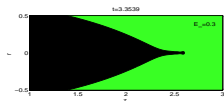
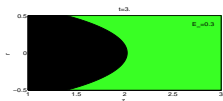




# Jet detail at breakup, $E_\infty = 0.40$



# Jet evolution details, $E_\infty = 0.3$ (horizontal view)



# Conclusions

1. By using the level set-boundary integral approach we have built up a seamless modeling and numerical methodology to study the evolution of a perfectly conducting droplet in a uniform electric field for various field strengths.
2. The numerical results obtained agree very well with previously published results up to the Taylor cone formation for uncharged droplets.
3. Our numerical method is also able to capture the jetting discharge for electric field values beyond the critical value and the long filaments ejected are in very good agreement with the Lab experiments of Grimm and Beauchamp.
4. The numerical model is prepared to handle multiple drops situations (axysimmetric) and there is a lot of work ahead to obtain results beyond beakup events.